APPENDIX A
RESULTS ON VOT-2019 AND VOT-2017 DATASET

A. *Evaluation on VOT-2019 dataset is given as follows:*

1) Fig. 1 shows the Expected Overlap Curves for baseline experiments
2) Fig. 2 shows the Expected Overlap Scores and Pooled AR plots.
3) Table I shows Accuracy values and Table II shows Robustness values of individual challenges for baseline experiments
4) Table III shows the Area under Overlap Curves of individual challenges for unsupervised experiments

B. *Evaluation on VOT-2017 dataset is given as follows:*

1) Fig. 3 shows the Accuracy-Robustness plots, Table IV shows Accuracy values and Table V shows Robustness values of individual challenges for baseline experiments
2) Fig. 4 shows the Expected Overlap Curves for baseline experiments
3) Fig. 5 shows the Expected Overlap Scores and Pooled Accuracy-Robustness (AR) plots.
4) Fig. 6 shows the Overlap Curves of individual challenges for unsupervised experiments
5) Table VI shows the Area under Overlap Curves of individual challenges for unsupervised experiments

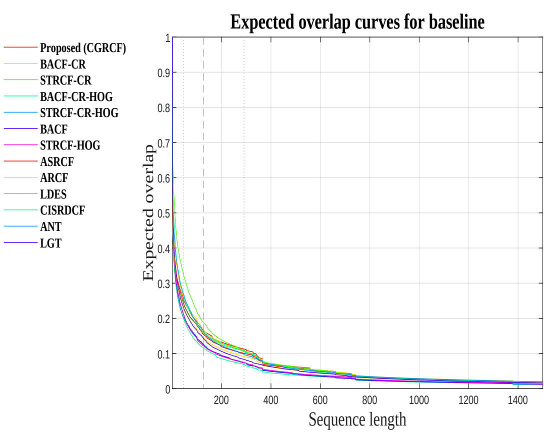

Fig. 1. Expected Overlap Curves for baseline experiments on VOT-2019 dataset

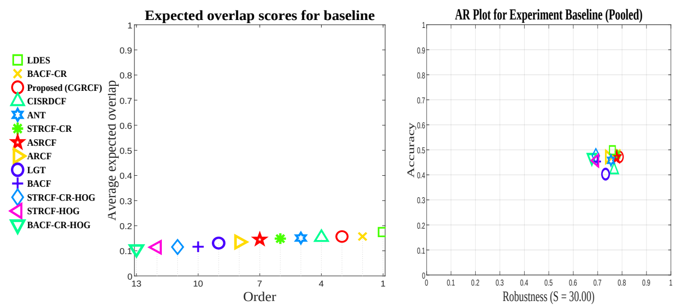

Fig. 2. Tracker ordering based on expected overlap score and pooled AR for baseline experiments on VOT-2019 dataset

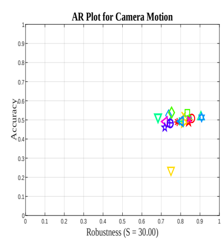

(a) Camera Motion

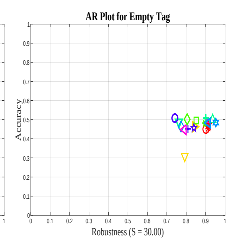

(b) Empty Tag

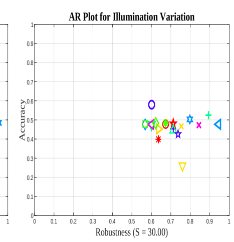

(c) Illumination Variation

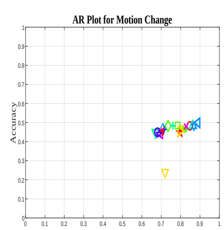

(d) Motion Change

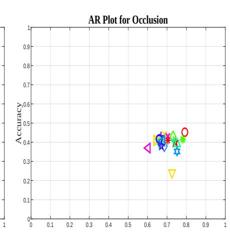

(e) Occlusion

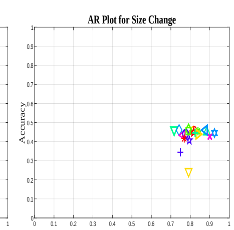

(f) Size Change

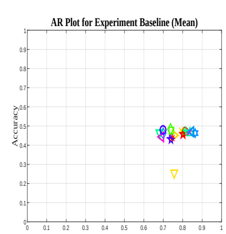

(g) Mean

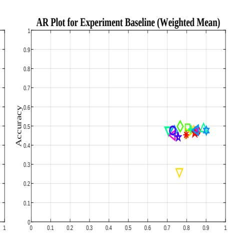

(h) Weighted Mean

Fig. 3. AR Plots of individual challenges for baseline experiments on VOT-2017 dataset

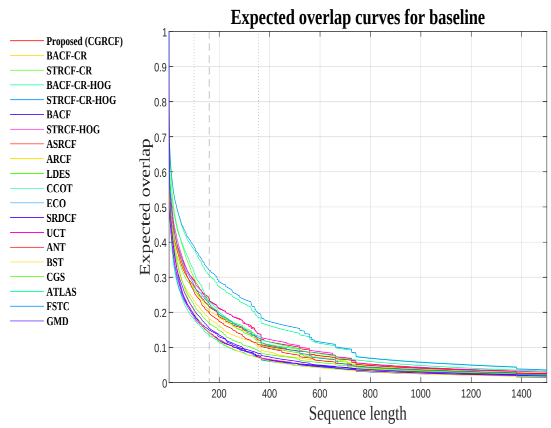

Fig. 4. Expected Overlap Curves for baseline experiments on VOT-2017 dataset

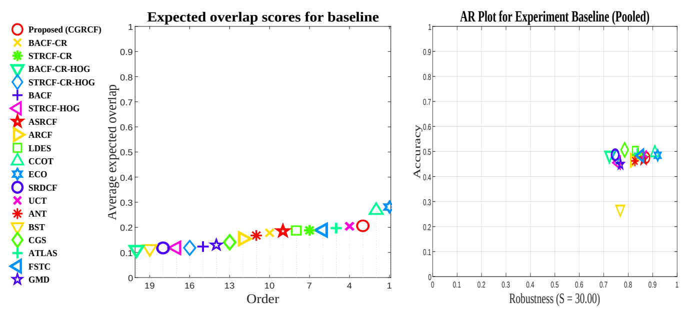

Fig. 5. Tracker ordering based on expected overlap score (left) and pooled Accuracy-Robustness (AR) plot that shows each tracker as a point in the joint AR rank space (right) for the baseline experiments on the VOT-2017 dataset.

TABLE I

ACCURACY COMPARISON OF THE PROPOSED APPROACHES WITH RECENT TRACKERS FOR THE BASELINE EXPERIMENT ON VOT-2019 DATASET. HERE CM = CAMERA MOTION, EMP = EMPTY TAG, IV= ILLUMINATION VARIATION, MC = MOTION CHANGE, OCC = OCCLUSION AND SC = SIZE CHANGE. HERE CM = CAMERA MOTION, EMP = EMPTY TAG, IV= ILLUMINATION VARIATION, MC = MOTION CHANGE, OCC = OCCLUSION AND SC = SIZE CHANGE. THE TOP THREE TRACKERS ARE SHOWN IN **RED**, **BLUE** AND **GREEN**.

	CM	EMP	IV	MC	OCC	SC	Mean	Weighted Mean	Average Pooled
Proposed (CGRCF)	0.4967	0.4487	0.4362	**0.4788**	**0.4483**	**0.4571**	**0.4610**	0.4698	0.4719
BACF-CR	**0.5106**	**0.4851**	**0.4391**	**0.4689**	**0.4333**	**0.4624**	**0.4666**	**0.4828**	**0.4868**
STRCF-CR	0.4997	**0.4853**	**0.4459**	0.4615	0.4089	0.4505	0.4586	**0.4746**	**0.4800**
BACF-CR-HOG	0.4866	0.4680	0.4388	0.4675	0.3828	0.4542	0.4496	0.4641	0.4690
STRCF-CR-HOG	**0.5121**	0.4650	0.4302	0.4634	0.3748	**0.4639**	0.4516	0.4711	0.4763
Correlation Filter based and Hybrid Trackers									
BACF [4]	0.4821	0.4546	0.4183	0.4607	**0.4306**	0.3290	0.4292	0.4476	0.4533
STRCF-HOG [5]	0.4789	0.4543	0.4353	0.4447	0.3746	0.4458	0.4389	0.4523	0.4570
ASRCF [1]	0.4825	0.4777	**0.4432**	0.4524	0.4003	0.4565	0.4521	0.4652	0.4707
ARCF [59]	0.4762	0.4842	0.4050	0.4637	0.4151	0.4515	0.4493	0.4669	0.4716
LDES [57]	**0.5321**	**0.4972**	0.4177	**0.4745**	0.4071	0.4330	**0.4603**	**0.4882**	**0.4986**
CISRDCF [13]	0.4201	0.4243	0.4224	0.4181	0.3853	0.3919	0.4104	0.4147	0.4198
ANT [13]	0.4906	0.4419	0.3650	0.4648	0.4187	0.3881	0.4282	0.4518	0.4581
LGT [13]	0.4067	0.4121	0.3752	0.3991	0.3879	0.3282	0.3849	0.3960	0.4030

TABLE II

ROBUSTNESS COMPARISON OF THE PROPOSED APPROACHES WITH RECENT TRACKERS FOR THE BASELINE EXPERIMENT ON VOT-2019 DATASET. HERE CM = CAMERA MOTION, EMP = EMPTY TAG, IV= ILLUMINATION VARIATION, MC = MOTION CHANGE, OCC = OCCLUSION AND SC = SIZE CHANGE. THE TOP THREE TRACKERS ARE SHOWN IN **RED**, **BLUE** AND **GREEN**.

	CM	EM	IV	MC	OCC	SC	Mean	Weighted Mean	Average Pooled
Proposed (CGRCF)	**53.00**	34.00	**9.00**	**64.00**	**22.00**	24.00	**34.33**	**42.16**	**157.00**
BACF-CR	**59.00**	**26.00**	**6.00**	70.00	31.00	23.00	**35.83**	**43.36**	**163.00**
STRCF-CR	**56.00**	**33.00**	**9.00**	**69.00**	**24.00**	**19.00**	**35.00**	**43.25**	**164.00**
BACF-CR-HOG	101.00	69.00	12.00	86.00	29.00	34.00	55.16	73.43	260.00
STRCF-CR-HOG	93.00	59.00	13.00	87.00	34.00	33.00	53.1667	68.38	244.00
Correlation Filter based and Hybrid Trackers									
BACF [4]	88.00	58.00	**9.00**	84.00	33.00	32.00	50.66	65.70	238.00
STRCF-HOG [5]	96.00	61.00	12.00	87.00	41.00	28.00	54.16	70.02	243.00
ASRCF [1]	60.00	**28.00**	**8.00**	72.00	28.00	25.00	36.83	44.58	167.00
ARCF [59]	65.00	47.00	11.00	74.00	40.00	**20.00**	42.83	52.71	197.00
LDES [57]	62.00	45.00	13.00	**66.00**	35.00	27.00	41.33	50.27	182.00
CISRDCF [13]	62.00	42.00	11.00	72.00	**27.00**	**22.00**	39.3333	48.98	176.00
ANT [13]	80.00	**28.00**	16.00	78.00	35.00	27.00	44.00	53.09	187.00
LGT [13]	77.11	39.44	11.20	79.80	28.65	24.80	43.50	54.86	206.85

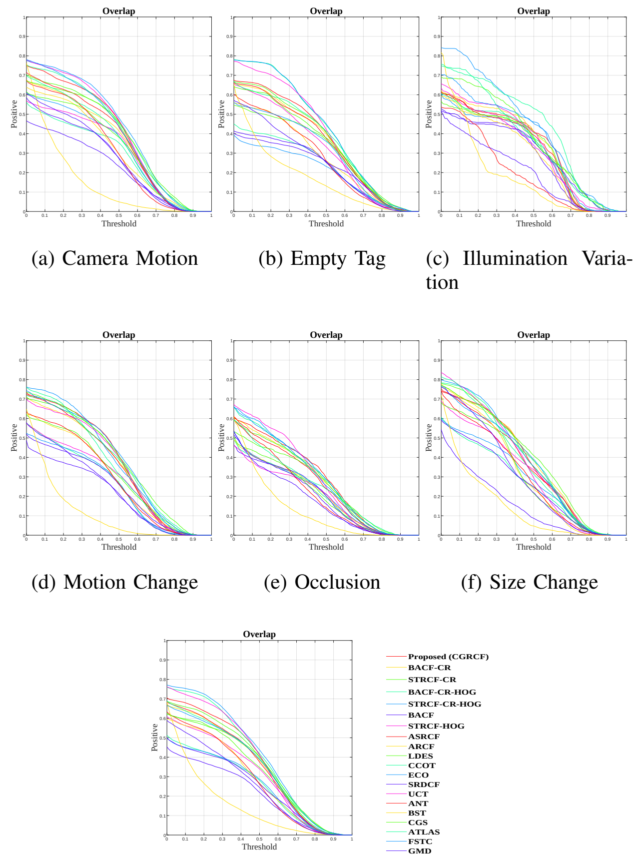

(a) Camera Motion (b) Empty Tag (c) Illumination Variation

(d) Motion Change (e) Occlusion (f) Size Change

(g) Average

Fig. 6. Curves of individual challenges for unsupervised experiments on VOT-2017 dataset

TABLE III

OVERLAP COMPARISON OF THE PROPOSED APPROACHES WITH RECENT TRACKERS FOR THE UNSUPERVISED EXPERIMENT ON VOT-2019 DATASET. HERE CM = CAMERA MOTION, EMP = EMPTY TAG, IV= ILLUMINATION VARIATION, MC = MOTION CHANGE, OCC = OCCLUSION AND SC = SIZE CHANGE. THE TOP THREE TRACKERS ARE SHOWN IN **RED**, **BLUE** AND **GREEN**.

	CM	**EMP**	**IV**	**MC**	**OCC**	**SC**	**Overall**
Proposed (CGRCF)	**0.3698**	**0.3343**	**0.2372**	**0.3176**	**0.2629**	**0.3306**	**0.3368**
BACF-CR	0.3329	0.3272	**0.2425**	0.2993	**0.2508**	**0.3449**	0.3184
STRCF-CR	**0.3522**	**0.3279**	0.2282	**0.3171**	**0.2468**	**0.3371**	**0.3273**
BACF-CR-HOG	0.2613	0.2454	0.2275	0.2175	0.2148	0.2228	0.2445
STRCF-CR-HOG	0.2999	0.1859	0.2056	0.2162	0.2048	0.2727	0.2365
Correlation Filter based and Hybrid Trackers							
BACF [4]	0.2171	0.2049	0.1779	0.1797	0.1787	0.1297	0.1959
STRCF-HOG [5]	0.3008	**0.3338**	0.2168	0.2481	0.1879	0.3160	0.2985
ASRCF [1]	**0.3446**	0.3268	0.2226	**0.3113**	0.2416	0.3303	**0.3230**
ARCF [59]	0.2923	0.2717	0.1873	0.2536	0.1949	0.2844	0.2690
LDES [57]	0.3131	0.3231	**0.2693**	0.2457	0.1887	0.2305	0.2940
CISRDCF [13]	0.2573	0.2382	0.1920	0.2054	0.2046	0.2055	0.2417
ANT [13]	0.2934	0.2088	0.1674	0.2269	0.1871	0.2210	0.2390
LGT [13]	0.2595	0.1981	0.1410	0.1773	0.1254	0.1968	0.2062

TABLE I

ACCURACY COMPARISON OF THE PROPOSED APPROACHES WITH RECENT TRACKERS FOR THE BASELINE EXPERIMENT ON VOT-2017 DATASET. HERE CM = CAMERA MOTION, EMP = EMPTY TAG, IV= ILLUMINATION VARIATION, MC = MOTION CHANGE, OCC = OCCLUSION AND SC = SIZE CHANGE. THE TOP THREE TRACKERS ARE SHOWN IN **RED**, **BLUE** AND **GREEN**.

	CM	EMP	IV	MC	OCC	SC	Mean	Weighted Mean	Average Pooled
Proposed (CGRCF)	0.5077	0.4503	0.4779	0.4828	**0.4524**	0.4585	0.4716	0.4737	0.4754
BACF-CR	**0.5262**	0.4804	0.4668	0.4748	**0.4420**	**0.4655**	0.4760	**0.4875**	0.4904
STRCF-CR	0.5085	0.4817	0.4831	0.4655	0.4148	0.4541	0.4680	0.4779	0.4825
BACF-CR-HOG	0.5153	0.4870	0.4753	0.4484	0.3999	**0.4615**	0.4646	0.4786	0.4846
STRCF-CR-HOG	0.5236	0.4638	0.4763	0.4656	0.3798	0.4603	0.4616	0.4741	0.4787
Correlation Filter based and Hybrid Trackers									
BACF [4]	0.4845	0.4515	0.4532	0.4638	**0.4339**	0.3440	0.4385	0.4476	0.4526
STRCF-HOG [5]	0.4912	0.4476	0.4758	0.4407	0.3698	0.4337	0.4431	0.4514	0.4552
ASRCF [1]	0.4906	0.4725	0.4809	0.4479	0.4010	0.4506	0.4572	0.4654	0.4701
ARCF [59]	0.4883	0.4633	0.4525	0.4551	0.4100	0.4393	0.4514	0.4615	0.4647
LDES [57]	**0.5370**	0.4956	0.4783	**0.4850**	0.4053	0.4559	0.4762	**0.4929**	**0.5023**
CCOT [37]	0.5158	0.4994	0.4460	**0.4835**	0.3917	0.4499	0.4644	0.4851	**0.4949**
ECO [17]	0.5131	0.4846	**0.5026**	0.4810	0.3520	0.4451	0.4631	0.4762	0.4848
SRDCF [3]	0.4816	**0.5080**	**0.5796**	0.4492	0.4171	0.4416	**0.4795**	0.4767	0.4867
UCT [12]	0.5026	0.4969	0.4726	0.4800	0.4312	0.4257	0.4681	0.4807	0.4887
ANT [12]	0.4890	0.4541	0.3986	0.4504	0.4099	0.4166	0.4364	0.4540	0.4622
BST [12]	0.2376	0.3091	0.2606	0.2391	0.2412	0.2443	0.2553	0.2627	0.2697
CGS [12]	**0.5380**	**0.5018**	0.4831	0.4820	0.4289	**0.4632**	**0.4828**	**0.4979**	**0.5063**
ATLAS [12]	0.4926	**0.5079**	**0.5248**	0.4830	0.4098	0.4449	**0.4772**	0.4835	0.4916
FSTC [12]	0.4926	0.4826	0.4770	**0.4986**	0.4076	0.4604	0.4698	0.4783	0.4836
GMD [12]	0.4607	0.4573	0.4258	0.4411	0.3801	0.4072	0.4287	0.4422	0.4490

TABLE II

ROBUSTNESS COMPARISON OF THE PROPOSED APPROACHES WITH RECENT TRACKERS FOR THE BASELINE EXPERIMENT ON VOT-2017 DATASET. HERE CM = CAMERA MOTION, EMP = EMPTY TAG, IV= ILLUMINATION VARIATION, MC = MOTION CHANGE, OCC = OCCLUSION AND SC = SIZE CHANGE. THE TOP THREE TRACKERS ARE SHOWN IN **RED**, **BLUE** AND **GREEN**.

	CM	EMP	IV	MC	OCC	SC	Mean	Weighted Mean	Average Pooled
Proposed (CGRCF)	**40.00**	30.00	7.00	21.00	**18.00**	23.00	**23.16**	**29.23**	**97.00**
BACF-CR	53.00	27.00	5.00	28.00	29.00	25.00	27.83	34.26	118.00
STRCF-CR	44.00	31.00	7.00	25.00	**19.00**	20.00	24.33	31.01	105.00
BACF-CR-HOG	99.00	78.00	9.00	51.00	32.00	38.00	51.16	69.72	231.00
STRCF-CR-HOG	79.00	74.00	10.00	44.00	29.00	34.00	45.00	60.77	203.00
Correlation Filter based and Hybrid Trackers									
BACF [4]	77.00	61.00	6.00	43.00	31.00	33.00	41.83	55.77	189.00
STRCF-HOG [5]	85.00	68.00	9.00	46.00	39.00	31.00	46.33	61.33	198.00
ASRCF [1]	45.00	**26.00**	6.00	29.00	23.00	23.00	25.33	30.97	105.00
ARCF [59]	53.00	49.00	8.00	29.00	34.00	20.00	32.16	41.41	141.00
LDES [57]	47.00	46.00	10.00	31.00	27.00	27.00	32.00	39.64	133.00
CCOT [37]	**26.00**	**19.00**	6.00	**19.00**	**22.00**	**14.00**	**17.66**	**20.41**	**68.00**
ECO [17]	**25.00**	**14.00**	4.00	**18.00**	**22.00**	**9.00**	**15.33**	**17.66**	**59.00**
SRDCF [3]	76.00	86.00	9.00	49.00	32.00	29.00	46.83	64.11	208.00
UCT [12]	44.00	29.00	**3.00**	24.00	27.00	**12.00**	**23.16**	29.79	103.00
ANT [12]	64.00	**26.00**	8.00	45.00	27.00	30.00	33.33	40.15	135.00
BST [12]	74.73	66.93	4.86	41.93	24.66	26.73	39.97	55.50	188.60
CGS [12]	73.66	62.46	8.40	39.26	24.13	26.73	39.11	53.37	172.06
ATLAS [12]	60.00	30.00	**2.00**	35.00	24.00	22.00	28.83	37.42	127.00
FSTC [12]	57.00	**26.00**	**1.00**	**15.00**	30.00	15.00	24.00	31.95	114.00
GMD [12]	86.06	50.33	5.40	47.66	30.73	26.20	41.06	54.73	187.46

TABLE III

OVERLAP COMPARISON OF THE PROPOSED APPROACHES WITH RECENT TRACKERS FOR THE UNSUPERVISED EXPERIMENT ON VOT-2017 DATASET. HERE CM = CAMERA MOTION, EMP = EMPTY TAG, IV= ILLUMINATION VARIATION, MC = MOTION CHANGE, OCC = OCCLUSION AND SC = SIZE CHANGE. THE TOP THREE TRACKERS ARE SHOWN IN **RED**, **BLUE** AND **GREEN**.

	CM	EMP	IV	MC	OCC	SC	Overall
Proposed (CGRCF)	0.3868	0.3577	0.3229	0.3603	**0.2769**	0.3557	0.3621
BACF-CR	0.3426	0.3470	0.3264	0.3425	0.2642	**0.3673**	0.3414
STRCF-CR	0.3654	0.3534	0.3130	0.3599	0.2610	0.3596	0.3530
BACF-CR-HOG	0.2752	0.2258	0.3079	0.2442	0.1936	0.2536	0.2454
STRCF-CR-HOG	0.3133	0.1984	0.2932	0.2417	0.2026	0.2770	0.2474
Correlation Filter based and Hybrid Trackers							
BACF [4]	0.2196	0.2204	0.2649	0.2021	0.1809	0.1472	0.2083
STRCF-HOG [5]	0.3046	0.3183	0.2971	0.2708	0.1884	0.3142	0.3006
ASRCF [1]	0.3583	0.3419	0.3083	0.3452	0.2511	0.3401	0.3411
ARCF [59]	0.3055	0.2735	0.2781	0.2836	0.1989	0.3046	0.2824
LDES [57]	0.3302	0.3405	**0.3648**	0.2988	0.1985	0.2929	0.3237
CCOT [37]	**0.4002**	**0.4113**	0.3618	0.3386	**0.2767**	0.3532	**0.3909**
ECO [17]	**0.4189**	**0.4132**	**0.4251**	**0.3701**	**0.2804**	**0.3695**	**0.4025**
SRDCF [3]	0.2606	0.2230	0.2901	0.2417	0.1990	0.2534	0.2445
UCT [12]	**0.4015**	**0.3801**	0.3283	0.3472	0.2760	0.3446	**0.3736**
ANT [12]	0.3036	0.2681	0.1910	0.2822	0.2047	0.2909	0.2770
BST [12]	0.1411	0.1678	0.1720	0.1067	0.1194	0.1391	0.1458
CGS [12]	0.3773	0.3014	0.3154	**0.3722**	0.2497	**0.3846**	0.3386
ATLAS [12]	0.3411	0.3524	**0.4237**	0.3666	0.2370	0.3669	0.3431
FSTC [12]	0.3905	0.2970	0.3541	**0.3696**	0.2727	0.3488	0.3359
GMD [12]	0.2707	0.2486	0.1932	0.2262	0.1683	0.2886	0.2492

Appendix B
Complete Derivation For *BACF-channel Regularized* and *STRCF-Channel Regularized*

A. BACF-Channel Regularized

To learn appropriate weights for each of the K responses, $\mathbf{x}_k * (\mathbf{P}^T\mathbf{h}_k)$ in (1) from the main manuscript, we propose the following BACF-Channel Regularized (BACF-CR) formulation,

$$E(\mathbf{h},\mathbf{q}) = \frac{1}{2}\left\|\mathbf{y} - \sum_{k=1}^{K} q_k(\mathbf{x}_k * (\mathbf{P}^T\mathbf{h}_k))\right\|_2^2 + \frac{\lambda}{2}\sum_{k=1}^{K}\|\mathbf{h}_k\|_2^2 + \frac{\beta}{2}\|\mathbf{q}\|_2^2, \tag{3}$$

where q_k is a scalar weight for response channel k, β is the regularization parameter, $\mathbf{q} = \{q_1, q_2, ..., q_K\}$, and $\frac{\beta}{2}\|\mathbf{q}\|_2^2$ is a regularization term for channel weights. Inspired by many previous works to achieve computational efficiency, we use Parseval's theorem to express (3) in the frequency domain [1], [4], [5], [3]. The equality constrained optimization form of (3) is given by,

$$E(\hat{\mathbf{G}},\mathbf{H},\mathbf{q}) = \frac{1}{2}\left\|\hat{\mathbf{y}} - \sum_{k=1}^{K}(\hat{\mathbf{x}}_k \odot \hat{\mathbf{g}}_k)\right\|_2^2 + \frac{\lambda}{2}\sum_{k=1}^{K}\|\mathbf{h}_k\|_2^2 + \frac{\beta}{2}\|\mathbf{q}\|_2^2$$
$$s.t.,\ \hat{\mathbf{g}}_k = \sqrt{T}\mathbf{F}\mathbf{P}^T\mathbf{h}_k q_k, \text{ and } \hat{\mathbf{x}}_k = \sqrt{T}\mathbf{F}\mathbf{x}_k,\quad k = 1,2,...,K, \tag{4}$$

where $\hat{}$ denotes the Discrete Fourier Transform (DFT) of a signal, such that $\hat{\mathbf{a}} = \sqrt{T}\mathbf{F}\mathbf{a}$, $\mathbf{a} \in \mathbb{R}^{T\times 1}$, $\mathbf{H} = [\mathbf{h}_1, \mathbf{h}_2, ..., \mathbf{h}_K]$, $\mathbf{F}$ is a $T \times T$ orthonormal matrix of complex basis vectors that transforms any T dimensional vectorized signal into the Fourier domain and $\hat{\mathbf{G}} = [\hat{\mathbf{g}}_1, \hat{\mathbf{g}}_2, ..., \hat{\mathbf{g}}_K]$ is an auxiliary variable matrix in the Fourier domain.

Using Parseval's theorem, the energy can equivalently be represented in the time or frequency domain. Therefore, the last two terms in (3) are equivalent to their Fourier counterparts and since they are used only to obtain the Fourier domain filter $\hat{\mathbf{g}}$, we do not convert them to the Fourier domain in (4). Further, they can efficiently be solved in the time domain itself. We introduce an auxiliary variable, $\mathbf{G}$, to obtain the decomposition of $E(\mathbf{H},\mathbf{q})$ in a form which can be efficiently solved using ADMM iterations [48]. It leads to decoupling between $\hat{\mathbf{G}}, \mathbf{H}$ and $\mathbf{q}$, where $\hat{\mathbf{G}}, \mathbf{H}$ and $\mathbf{q}$ can also be solved using ADMM iterations [48]. The augmented Lagrangian form of (4) can be written as,

$$E(\hat{\mathbf{G}},\mathbf{H},\mathbf{q},\hat{\mathbf{S}}) = \frac{1}{2}\left\|\hat{\mathbf{y}} - \sum_{k=1}^{K}\hat{\mathbf{x}}_k \odot \hat{\mathbf{g}}_k\right\|_2^2 + \frac{\lambda}{2}\sum_{k=1}^{K}\|\mathbf{h}_k\|_2^2 + \frac{\mu}{2}\sum_{k=1}^{K}\left\|\hat{\mathbf{g}_k} - \sqrt{T}\mathbf{F}\mathbf{P}^T\mathbf{h}_k q_k + \frac{\hat{\mathbf{s}}_k}{\mu}\right\|_2^2 + \frac{\beta}{2}\|\mathbf{q}\|_2^2, \tag{5}$$

where μ is the penalty factor and $\hat{\mathbf{S}} = [\hat{\mathbf{s}}_1, \hat{\mathbf{s}}_2, ..., \hat{\mathbf{s}}_K] \in \mathbb{R}^{T\times K}$ is the Fourier transform of the Lagrange multiplier. The above problem can be solved by using ADMM for the following sub-problems:

Solving for H: Given $\hat{\mathbf{G}}, \mathbf{q}$ and $\hat{\mathbf{S}}$ in (5), the optimal solution for $\mathbf{H}^*$ can be obtained by,

$$\mathbf{h}_k^* = \underset{\mathbf{h}_k}{\operatorname{argmin}} \frac{\lambda}{2}\sum_{k=1}^{K}\|\mathbf{h}_k\|_2^2 + \frac{\mu}{2}\sum_{k=1}^{K}\left\|\hat{\mathbf{g}_k} - \sqrt{T}\mathbf{F}\mathbf{P}^T\mathbf{h}_k q_k + \frac{\hat{\mathbf{s}}_k}{\mu}\right\|_2^2. \tag{6}$$

Computing the partial derivative with respect to $\mathbf{h}_k$ and equating to zero, we get,

$$\lambda\mathbf{h}_k - \mu\sqrt{T}\mathbf{P}\mathbf{F}^T q_k(\hat{\mathbf{g}}_k - \sqrt{T}\mathbf{F}\mathbf{P}^T\mathbf{h}_k q_k + \frac{\hat{\mathbf{s}}_k}{\mu}) = 0, \tag{7}$$

$$\lambda\mathbf{h}_k - \mu\sqrt{T}\mathbf{P}q_k\mathbf{F}^T\hat{\mathbf{g}}_k + \mu T\mathbf{P}\mathbf{P}^T q_k^2\mathbf{h}_k - \sqrt{T}\mathbf{P}\mathbf{F}^T\hat{\mathbf{s}}_k q_k = 0, \tag{8}$$

$$\lambda\mathbf{h}_k - \mu T\mathbf{P}q_k\mathbf{g}_k + \mu T\mathbf{P}\mathbf{P}^T q_k^2\mathbf{h}_k - Tq_k\mathbf{P}\mathbf{s}_k = 0, \tag{9}$$

$$(\lambda\mathbf{I} + \mu T\mathbf{P}\mathbf{P}^T q_k^2)\mathbf{h}_k = Tq_k\mathbf{P}(\mu\mathbf{g}_k + \mathbf{s}_k), \tag{10}$$

$$\mathbf{h}_k^* = (\lambda\mathbf{I} + \mu T\mathbf{P}\mathbf{P}^T q_k^2)^{-1}Tq_k\mathbf{P}(\mu\mathbf{g}_k + \mathbf{s}_k), \tag{11}$$

where $\mathbf{I}$ is a $T \times T$ identity matrix and the inverse term can be efficiently obtained by computing the reciprocal of each element.

Solving for $\hat{\mathbf{G}}$: Fixing $\mathbf{H}$, $\mathbf{q}$ and $\hat{\mathbf{S}}$ in (5), the optimal $\hat{\mathbf{G}}^*$ can be obtained by solving,

$$\hat{\mathbf{G}}^* = \underset{\hat{\mathbf{G}}}{\operatorname{argmin}} \frac{1}{2}\left\|\hat{\mathbf{y}} - \sum_{k=1}^{K}\hat{\mathbf{x}}_k \odot \hat{\mathbf{g}}_k\right\|_2^2 + \frac{\mu}{2}\sum_{k=1}^{K}\left\|\hat{\mathbf{g}_k} - \sqrt{T}\mathbf{F}\mathbf{P}^T\mathbf{h}_k q_k + \frac{\hat{\mathbf{s}}_k}{\mu}\right\|_2^2. \tag{12}$$

However, due to high computational complexity, it is difficult to optimize (12) [1]. Therefore, we process pixel-wise for all channels. The reformulated optimization problem in (12) is given by,

$$\mathcal{V}_j^*(\hat{\mathbf{G}}) = \underset{\mathcal{V}_j(\mathbf{G})}{\operatorname{argmin}} \frac{1}{2}\left\|\hat{\mathbf{y}}_j - \mathcal{V}_j(\hat{\mathbf{X}})^T\mathcal{V}_j(\hat{\mathbf{G}})\right\|_2^2 + \frac{\mu}{2}\sum_{k=1}^{K}\left\|\mathcal{V}_j(\hat{\mathbf{G}}) + \mathcal{V}_j(\hat{\mathbf{M}})\right\|_2^2, \tag{13}$$

where $\mathbf{X} = [\mathbf{x}_1, \mathbf{x}_2, ..., \mathbf{x}_K]$ and $\hat{\mathbf{X}} = [\hat{\mathbf{x}}_1, \hat{\mathbf{x}}_2, ..., \hat{\mathbf{x}}_K]$. $\mathcal{V}_j(\hat{\mathbf{X}}) = [\hat{\mathbf{x}}_{1j}, \hat{\mathbf{x}}_{2j} ..., \hat{\mathbf{x}}_{Kj}]^T$ is a $K \times 1$ vector, picking the j^{th} element from each channel of $\hat{\mathbf{X}}$, i.e., $\mathcal{V}_1(\hat{\mathbf{X}}) = [\hat{\mathbf{x}}_{11}, \hat{\mathbf{x}}_{21}, ..., \hat{\mathbf{x}}_{K1}]^T$ and $\mathcal{V}_j(\hat{\mathbf{G}}) = [\hat{\mathbf{g}}_{1j}, \hat{\mathbf{g}}_{2j}, ..., \hat{\mathbf{g}}_{Kj}]^T$. Similarly, we form,

$$\mathcal{V}_j(\hat{\mathbf{M}}) = \mathcal{V}_j\left(\frac{\hat{\mathbf{S}}}{\mu}\right) - \mathcal{V}_j(\sqrt{T}\mathbf{F}\mathbf{P}^T\mathbf{H}\mathbf{q}),$$

where $\mathcal{V}_j\left(\frac{\hat{\mathbf{S}}}{\mu}\right) = [\frac{\hat{\mathbf{s}}_{1j}}{\mu}, \frac{\hat{\mathbf{s}}_{2j}}{\mu}, ..., \frac{\hat{\mathbf{s}}_{kj}}{\mu}]^T$. Solving (13), we get,

$$[\mu\mathbf{I} + \mathcal{V}_j(\hat{\mathbf{X}})\mathcal{V}_j(\hat{\mathbf{X}})^T]\mathcal{V}_j(\hat{\mathbf{G}}) = \hat{\mathbf{y}}_j\mathcal{V}_j(\hat{\mathbf{X}}) - \mu\mathcal{V}_j(\hat{\mathbf{M}}),$$

$$\mathcal{V}_j^*(\hat{\mathbf{G}}) = (\mu\mathbf{I} + \mathcal{V}_j(\hat{\mathbf{X}})\mathcal{V}_j(\hat{\mathbf{X}})^T)^{-1}$$
$$(\hat{\mathbf{y}}_j\mathcal{V}_j(\hat{\mathbf{X}}) - \mu\mathcal{V}_j\left(\frac{\hat{\mathbf{S}}}{\mu}\right) + \mu\mathcal{V}_j(\sqrt{T}\mathbf{F}\mathbf{P}^T\mathbf{H}\mathbf{q})), \tag{14}$$

where $\mathbf{q} = \{q_1, q_2, ..., q_K\}$ and $\mathbf{H} = [\mathbf{h}_1, \mathbf{h}_2, ..., \mathbf{h}_K]$. Equation (14) can be efficiently computed using the Sherman-Morrison formula [1] as follows.

$$\mathcal{V}_j^*(\hat{\mathbf{G}}) = \frac{1}{\mu}\left(\mathbf{I} - \frac{\mathcal{V}_j(\hat{\mathbf{X}})\mathcal{V}_j(\hat{\mathbf{X}})^T}{\mu + \mathcal{V}_j(\hat{\mathbf{X}})^T\mathcal{V}_j(\hat{\mathbf{X}})}\right)(\hat{\mathbf{y}}_j\mathcal{V}_j(\hat{\mathbf{X}}) -$$
$$\mu\mathcal{V}_j\left(\frac{\hat{\mathbf{S}}}{\mu}\right) + \mu\mathcal{V}_j(\sqrt{T}\mathbf{F}\mathbf{P}^T\mathbf{H}\mathbf{q})). \tag{15}$$

Solving for q_k*:* If $\hat{\mathbf{G}}$, $\mathbf{H}$ and $\hat{\mathbf{S}}$ are fixed in (5), q_k can be computed as follows,

$$q_k^* = \underset{q_k}{\operatorname{argmin}}\, \frac{\mu}{2}\sum_{k=1}^{K}\left\|\hat{\mathbf{g}_k} - \sqrt{T}\mathbf{F}\mathbf{P}^T\mathbf{h}_k q_k + \frac{\hat{\mathbf{s}}_k}{\mu}\right\|_2^2 + \frac{\beta}{2}\|\mathbf{q}\|_2^2. \tag{16}$$

Solving (16), we get,

$$(\mu\sqrt{T}\mathbf{h}_k{}^T\mathbf{P}\mathbf{P}^T\mathbf{h}_k + \beta)q_k = \mu\sqrt{T}\mathbf{h}_k{}^T\mathbf{P}\mathbf{g}_k + T\mathbf{h}_k{}^T\mathbf{P}\mathbf{s}_\mathbf{k},$$
$$q_k^* = \frac{\mu\sqrt{T}\mathbf{h}_k{}^T\mathbf{P}\mathbf{g}_k + T\mathbf{h}_k{}^T\mathbf{P}\mathbf{s}_\mathbf{k}}{\mu\sqrt{T}\mathbf{h}_k{}^T\mathbf{P}\mathbf{P}^T\mathbf{h}_k + \beta}. \tag{17}$$

B. STRCF-Channel Regularized

For each of the K responses, $(\mathbf{x}_k * \mathbf{h}_k)$ in (2), we learn an appropriate weight using the following STRCF-Channel Regularized (STRCF-CR) formulation,

$$E(\mathbf{h}, \mathbf{q}) = \frac{1}{2}\left\|\mathbf{y} - \sum_{k=1}^{K} q_k(\mathbf{x}_k * \mathbf{h}_k)\right\|_2^2 + \frac{1}{2}\sum_{k=1}^{K}\|\mathbf{w}\odot\mathbf{h}_k\|_2^2 +$$
$$\frac{\theta}{2}\sum_{k=1}^{K}\left\|\mathbf{h}_k^{(t)} - \mathbf{h}_k^{(t-1)}\right\|_2^2 + \frac{\beta}{2}\|\mathbf{q}\|_2^2. \tag{18}$$

Here, $\mathbf{w}$ is the spatial regularization matrix [5]. In the forthcoming equations, the notation follows the previous section unless mentioned otherwise. Using Parseval's theorem to express (18) in the frequency domain, the equality constrained optimization form is,

$$E(\hat{\mathbf{G}}, \mathbf{H}, \mathbf{q}) = \frac{1}{2}\left\|\hat{\mathbf{y}} - \sum_{k=1}^{K}\hat{\mathbf{x}}_k\odot\hat{\mathbf{g}}_k\right\|_2^2 + \frac{1}{2}\sum_{k=1}^{K}\|\mathbf{w}\odot\mathbf{h}_k\|_2^2 +$$
$$\frac{\theta}{2}\sum_{k=1}^{K}\left\|\mathbf{h}_k^{(t)} - \mathbf{h}_k^{(t-1)}\right\|_2^2 + \frac{\beta}{2}\|\mathbf{q}\|_2^2,$$
$$s.t.,\ \hat{\mathbf{g}}_k = \sqrt{T}\mathbf{F}\mathbf{h}_k q_k. \tag{19}$$

Similar to BACF-CR, the local optimum solution to the model in (19) can be obtained using ADMM. The augmented Lagrangian form of (19) can be written as,

$$E(\hat{\mathbf{G}}, \mathbf{H}, \mathbf{q}, \hat{\mathbf{S}}) = \frac{1}{2}\left\|\hat{\mathbf{y}} - \sum_{k=1}^{K}\hat{\mathbf{x}}_k\odot\hat{\mathbf{g}}_k\right\|_2^2 + \frac{1}{2}\sum_{k=1}^{K}\|\mathbf{w}\odot\mathbf{h}_k\|_2^2 +$$
$$\frac{\theta}{2}\sum_{k=1}^{K}\left\|\mathbf{h}_k^{(t)} - \mathbf{h}_k^{(t-1)}\right\|_2^2 + \frac{\mu}{2}\sum_{k=1}^{K}\left\|\hat{\mathbf{g}_k} - \sqrt{T}\mathbf{F}\mathbf{h}_k q_k + \frac{\hat{\mathbf{s}}_k}{\mu}\right\|_2^2 +$$
$$\frac{\beta}{2}\|\mathbf{q}\|_2^2. \tag{20}$$

The above problem can be solved using ADMM for the following sub-problems:

Solving for H*:* Given $\hat{\mathbf{G}}, \mathbf{q}$ and $\hat{\mathbf{S}}$ in (20), the optimal solution for $\mathbf{H}^*$ can be obtained by,

$$\mathbf{h}_k^* = \underset{\mathbf{h}_k}{\operatorname{argmin}}\, \frac{1}{2}\sum_{k=1}^{K}\|\mathbf{w}\odot\mathbf{h}_k\|_2^2 + \frac{\theta}{2}\sum_{k=1}^{K}\left\|\mathbf{h}_k^{(t)} - \mathbf{h}_k^{(t-1)}\right\|_2^2 +$$
$$\frac{\mu}{2}\sum_{k=1}^{K}\left\|\hat{\mathbf{g}_k} - \sqrt{T}\mathbf{F}\mathbf{h}_k q_k + \frac{\hat{\mathbf{s}}_k}{\mu}\right\|_2^2. \tag{21}$$

Solving (21), we get,

$$\mathbf{h}_k^* = (\lambda\mathbf{W}\mathbf{W}^T + \mu T q_k^2\mathbf{I} + \theta\mathbf{I})^{-1}(Tq_k(\mu\mathbf{g}_k + \mathbf{s}_k) + \theta\mathbf{h}_k^{(t-1)}), \tag{22}$$

where $\mathbf{W} = diag(\mathbf{w}) \in \mathbb{R}^{T\times T}$ and the inverse term can be conveniently obtained by computing the reciprocal of each element.

Solving for $\hat{\mathbf{G}}$*:* Fixing $\mathbf{H}, \mathbf{q}$ and $\hat{\mathbf{S}}$ in (20), the optimal $\hat{\mathbf{G}}^*$ can be obtained by solving,

$$\hat{\mathbf{G}}^* = \underset{\hat{\mathbf{G}}}{\operatorname{argmin}}\, \frac{1}{2}\left\|\hat{\mathbf{y}} - \sum_{k=1}^{K}\hat{\mathbf{x}}_k\odot\hat{\mathbf{g}}_k\right\|_2^2 +$$
$$\frac{\mu}{2}\sum_{k=1}^{K}\left\|\hat{\mathbf{g}_k} - \sqrt{T}\mathbf{F}\mathbf{h}_k q_k + \frac{\hat{\mathbf{s}}_k}{\mu}\right\|_2^2. \tag{23}$$

Equation (23) is solved using the same method that is used to solve (12). The analytical solution to (23) is given by,

$$\mathcal{V}_j^*(\hat{\mathbf{G}}) = \frac{1}{\mu}\left(\mathbf{I} - \frac{\mathcal{V}_j(\hat{\mathbf{X}})\mathcal{V}_j(\hat{\mathbf{X}})^T}{\mu + \mathcal{V}_j(\hat{\mathbf{X}})^T\mathcal{V}_j(\hat{\mathbf{X}})}\right)(\hat{\mathbf{y}}_j\mathcal{V}_j(\hat{\mathbf{X}}) -$$
$$\mu\mathcal{V}_j\left(\frac{\hat{\mathbf{S}}}{\mu}\right) + \mu\mathcal{V}_j(\sqrt{T}\mathbf{F}\mathbf{H}\mathbf{q})). \tag{24}$$

Solving for q_k*:* Given $\hat{\mathbf{G}}, \mathbf{H}$ and $\hat{\mathbf{S}}$ in (20), q_k is computed using,

$$q_k^* = \underset{q_k}{\operatorname{argmin}}\, \frac{\mu}{2}\sum_{k=1}^{K}\left\|\hat{\mathbf{g}_k} - \sqrt{T}\mathbf{F}\mathbf{h}_k q_k + \frac{\hat{\mathbf{s}}_k}{\mu}\right\|_2^2 + \frac{\beta}{2}\|\mathbf{q}\|_2^2. \tag{25}$$

Solving (25), we get,

$$(\mu\sqrt{T}\mathbf{h}_k{}^T\mathbf{h}_k + \beta)q_k = \mu\sqrt{T}\mathbf{h}_k{}^T\mathbf{g}_k + T\mathbf{h}_k{}^T\mathbf{s}_\mathbf{k},$$
$$q_k^* = \frac{\mu\sqrt{T}\mathbf{h}_k{}^T\mathbf{g}_k + T\mathbf{h}_k{}^T\mathbf{s}_\mathbf{k}}{\mu\sqrt{T}\mathbf{h}_k{}^T\mathbf{h}_k + \beta}. \tag{26}$$